[21]H. Sherif, Can. J. Phys. 49, 983 (1971).
[22]F. D. Becchetti, Jr., and G. W. Greenlees, Phys. Rev. 182, 1190 (1969).
[23]H. Sherif, Ph.D. thesis, University of Washington, 1968 (unpublished).
[24]H. Sherif and J. S. Blair, Phys. Letters 26B, 489 (1968).
[25]M. P. Fricke, R. M. Drisko, R. H. Bassel, E. E. Gross, B. V. Morton, and A. Zucker, Phys. Rev. Letters 16, 746 (1966).
[26]P. Kossanyi-Demay, R. de Swiniarski, and C. Glashausser, Nucl. Phys. A94, 513 (1967).
[27]C. Glashausser, R. de Swiniarski, and J. Thirion, Phys. Rev. 164, 1437 (1967).
[28]J. L. Escudié, J. C. Faivre, W. Haeberli, B. Mayer, and N. Poutcherov, Centre à l'Energie Atomique, Department de Physique Nucleaire, Compte Rendu d'Activité (unpublished).
[29]J. R. Tesmer, Ph.D. thesis, University of Washington, 1971 (unpublished).
[30]J. Raynal in *Proceedings of the Third International Symposium on Polarization Phenomena in Nuclear Reactions, Madison, 1970,* edited by H. H. Barschall and W. Haeberli (University of Wisconsin Press, Madison, Wisc., 1971).
[31]G. R. Satchler, in *Proceedings of the Third International Symposium on Polarization Phenomena in Nuclear Reactions* (see Ref. 30).

PHYSICAL REVIEW C VOLUME 5, NUMBER 3 MARCH 1972

Electromagnetic Transitions in V^{51} and Mn^{53}†

A. S. Goodman and D. J. Donahue
Department of Physics, University of Arizona, Tucson, Arizona 85721
(Received 7 October 1971)

Attenuated Doppler shifts and particle–γ-ray angular correlations have been measured and interpreted to yield properties of electromagnetic transitions in V^{51} and Mn^{53}. Mean lives have been obtained for states at 1.609, 1.813, 2.402, 2.670, and 2.699 MeV in V^{51}, and for states at 1.288, 1.440, 1.619, 2.277, 2.406, 2.575, 2.641, and 2.705 MeV in Mn^{53}. Possible multipole mixing ratios have been deduced for the transitions (energies in MeV) $0.378 \rightarrow 0$, $1.288 \rightarrow 0.378$, $1.619 \rightarrow 0$, $2.277 \rightarrow 0$, and $2.406 \rightarrow 1.288$ in Mn^{53}. A possible identification of a $\frac{15}{2}^-$ state in Mn^{53} is presented. From these results and the results of other workers, transition probabilities in V^{51} and Mn^{53} have been calculated and compared (i) with one another, (ii) with a $(1f_{7/2})^n$ pure-configuration shell-model calculation, and (iii) with a mixed-configuration calculation.

I. INTRODUCTION

In a simple shell-model picture, the nuclei $_{23}V^{51}$ and $_{25}Mn^{53}$ can be considered to contain a closed shell of 28 neutrons and, respectively, three protons and three proton holes in the $1f_{7/2}$ shell. There are several predictions of the pure-configuration shell-model calculation[1] which make an investigation of the electromagnetic transitions among states of these nuclei of interest. First, since all electromagnetic transitions among $(1f_{7/2})^n$ states would be between states of the same j shell, the pure-configuration model predicts that all dipole transitions are strictly forbidden. Second, since the model treats particles and holes equivalently, transition probabilities in the two nuclei should be identical. Third, calculations have recently been made[2] which indicate that many $E2$ transition probabilities in the $1f_{7/2}$ shell can be predicted with a single assumption concerning the effective charge of the neutrons and protons in this shell. Finally, in addition to the pure-configuration calculations, mean lives of states in Mn^{53} have recently been obtained from calculations[3] which include contributions from single-particle levels other than the $1f_{7/2}$ shell.

In the work presented here, some electromagnetic transition probabilities for the two nuclei have been measured and compared with predictions using both the simple and the more complicated model. We have used the reactions $Ti^{48}(\alpha, p\gamma)V^{51}$ and $Cr^{50}(\alpha, p\gamma)Mn^{53}$ to study the level structure and mean lives for states up to 2.7 MeV in V^{51}, and the level structure, decay scheme, lifetimes, multipole mixing ratios, and branching ratios, where possible, for states up to 2.705 MeV in Mn^{53}. Mean-life measurements in both cases were made using a p-γ coincidence version of the Doppler-shift-attenuation method.[4] Multipole mixing ratios in Mn^{53} were determined by observing the angular correlations between protons from the reaction $Cr^{50}(\alpha, p\gamma)Mn^{53}$ and the emitted γ rays. This technique is described by Litherland and Ferguson as method II.[5]

A considerable amount of prior information about these nuclei is available. Horoshko, Cline, and Lesser[6] have measured branching ratios, $B(E2)$'s, and multipole mixing ratios in V^{51}. Brandolini, Brusegan, Ricci, and Signorini[7] measured mean lives of three states in Mn^{53}. McEllistrem, Jones, and Shephard,[8] Vuister,[9] and Goredetzky, Beck, Bertini, Bozek, and Knipper[10] have measured some multipole mixing ratios in Mn^{53}. In addition, Szöghy, Cujec, and Dayras[11] used the same reaction that we have, $Cr^{50}(\alpha,p\gamma)Mn^{53}$, to measure branching ratios and proton–γ-ray correlations in Mn^{53}. Our branching-ratio and multipole-mixing-ratio measurements in Mn^{53} complement those of Szöghy *et al.*, and our measurements of mean lives allow a fairly comprehensive study of transition rates in V^{51} and Mn^{53} to be made.

II. EXPERIMENTAL METHOD

α particles were produced by accelerating helium ions in the University of Arizona 5.5-MV Van de Graaff, and extracting the doubly ionized helium beam. α-particle energies ranged from 9 to 10 MeV. Targets were produced by vacuum-deposition techniques, and areal densities were determined by direct weight measurements. Target-backing material was 0.010-in. tantalum. Three different targets were used for the reaction $Ti^{48}(\alpha,p\gamma)V^{51}$. Two of these were prepared from natural, pure, titanium metal (74% Ti^{48}) with areal densities of 350 ± 40 and 450 ± 50 $\mu g/cm^2$. The third was prepared from TiO_2 enriched to 99.1% Ti^{48}, and had an areal density of 230 ± 30 $\mu g/cm^2$. Only one target was used for the reaction $Cr^{50}(\alpha,p\gamma)Mn^{53}$. This was prepared from metallic chromium enriched to 95.9% Cr^{50}. The areal density of this target was 250 ± 40 $\mu g/cm^2$.

A. Doppler-Shift-Attenuation Method

We used the p-γ coincidence version of the Doppler-shift-attenuation method, with collinear geometry as described in detail by Hershberger, Wozniak, and Donahue.[4] Analysis of data and error analysis for these experiments follow the methods described previously.[12] Differences in energies of Doppler-shifted γ rays, $\Delta(E_\gamma)_{meas}$, are determined by measuring simultaneously the energies of γ rays emitted by the decaying nuclei in two directions relative to the direction of recoil. These energies are determined from the data by calculating peak centroids. Errors in peak centroids and the differences, are determined by standard statistical techniques. These differences in energies of Doppler-shifted γ rays were used to obtain an experimental attenuation factor, F, given by

$$F_{expt} = \Delta\langle E_\gamma\rangle_{meas}/\Delta\langle E_\gamma\rangle_0 , \quad (1)$$

where $\Delta\langle E_\gamma\rangle_0$ is the calculated unattenuated energy difference; i.e., the difference in energy of γ rays from nuclei which are not slowed down. The calculations of $\Delta\langle E_\gamma\rangle_0$ took into account the range of velocities of the recoiling nuclei resulting from the finite size of the proton detectors used to determine the p-γ coincidence condition, and the appropriate averages over the finite size of the γ-ray detector. Experimental attenuation factors were then compared with attenuation factors calculated for various values of τ, and mean lives read from the plotted F_{calc} versus τ curves. Stopping powers used in the calculation of F_{calc} were determined from the theory of Lindhard, Scharff, and Schiøtt,[13] with the modifications suggested by Blaugrund[14] to account for large-angle nuclear

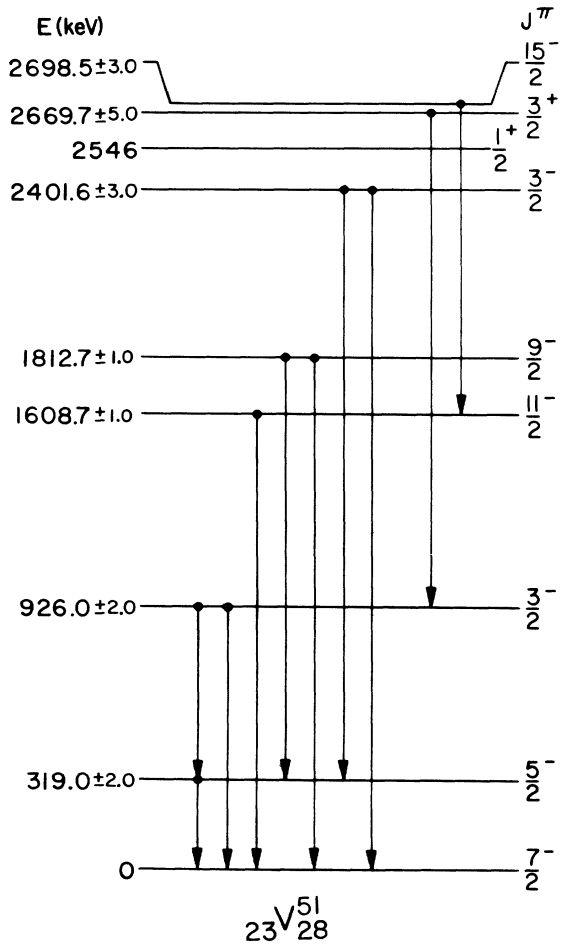

FIG. 1. Energy-level diagram for V^{51}. All known levels below 2.7 MeV are indicated. The γ-ray transitions shown are those observed in this work.

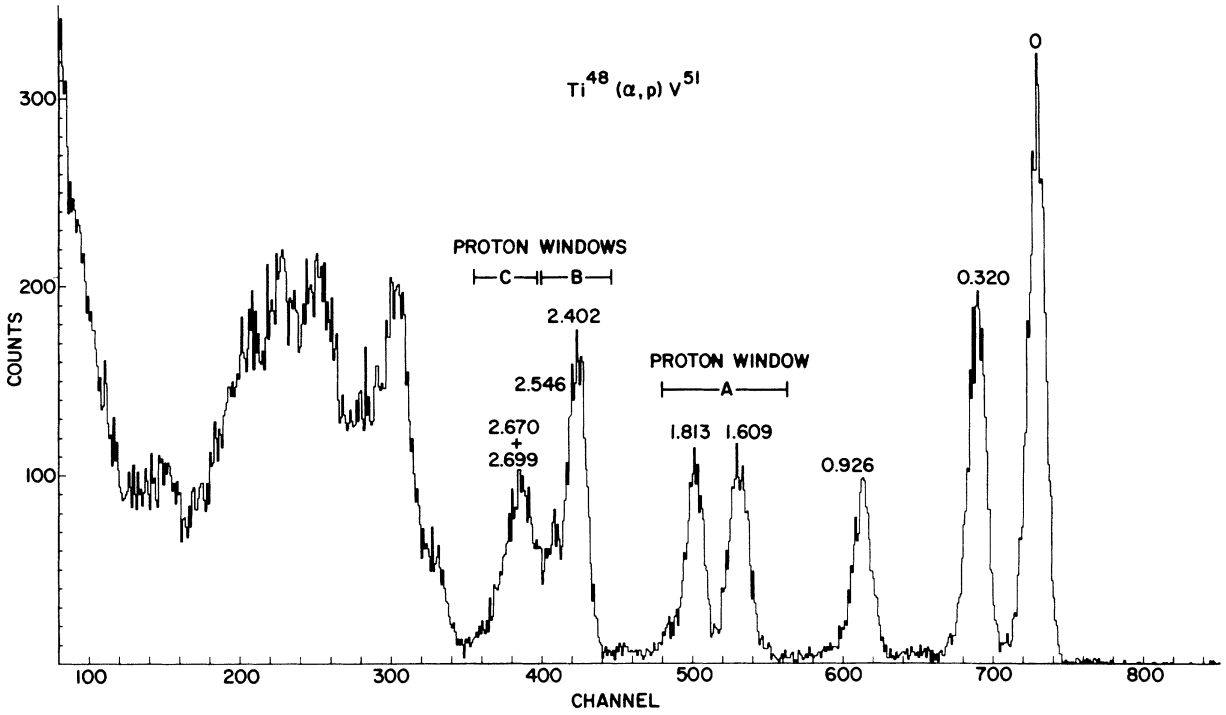

FIG. 2. Proton spectrum from the $Ti^{48}(\alpha, p)V^{51}$ reaction. The incident α-particle energy was 9.2 MeV and the target was Ti^{48} enriched TiO_2 with an areal density of 230 $\mu g/cm^2$. Peaks are labeled with V^{51} level energies. Proton windows used in the Doppler-shift-attenuation measurements are labeled.

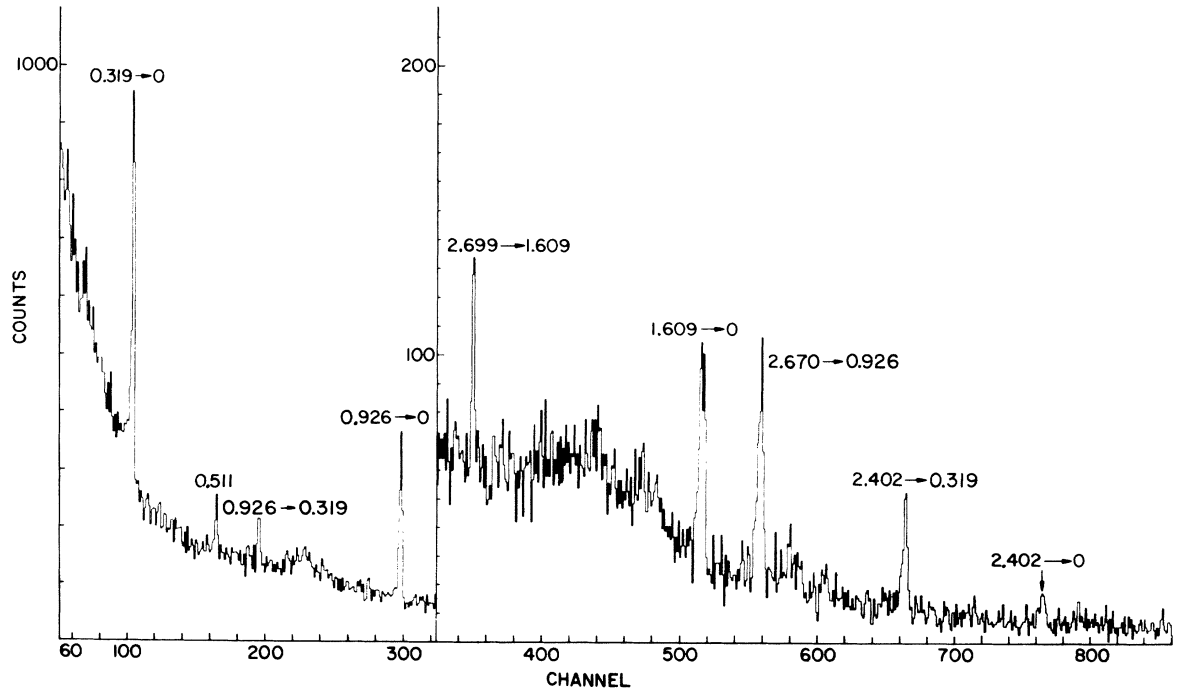

FIG. 3. Coincident γ-ray spectrum for V^{51}. These data were taken using γ rays in coincidence with protons from the downstream target only. Proton window C (see Fig. 2) was used to obtain this spectrum.

scattering. Uncertainties in stopping powers were assumed to be 20%.

B. Angular-Correlation Measurements

We have used the method of angular correlations described by Litherland and Ferguson[5] as method II. The reaction $Cr^{50}(\alpha, p\gamma)Mn^{53}$ was used with α-particle energies of 9.6 (for the 0.317-MeV state) and 9.1 MeV. The reaction protons were detected in a 300-mm^2 annular silicon surface-barrier detector located 25.4 mm from the target. The scattering angles subtended by the proton detector were between 164 and 175° with respect to the in-

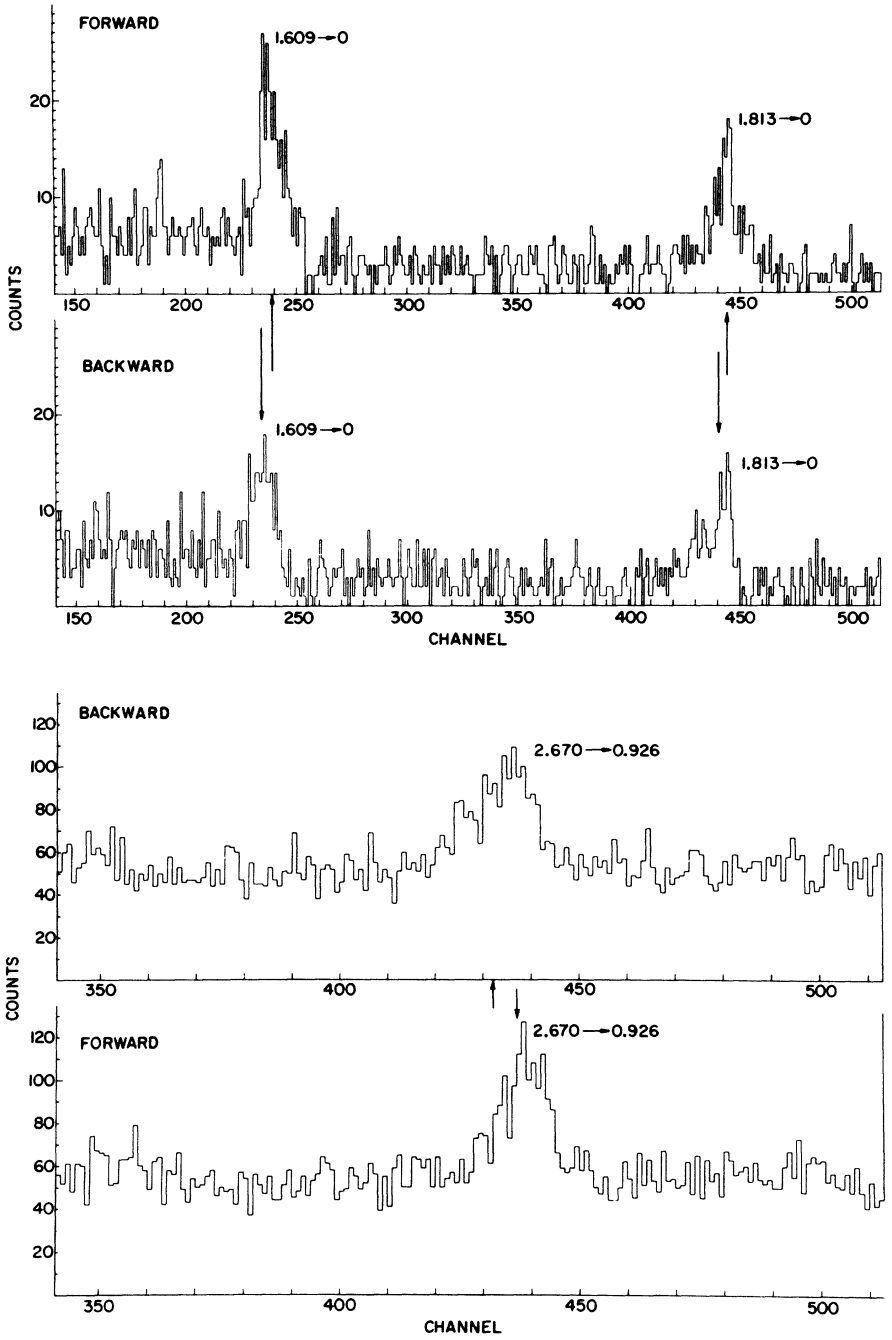

FIG. 4. Coincident γ-ray spectra for V^{51} for the transitions 1.813 MeV → 0, 1609 MeV → 0, and 2.670 → 0.930 MeV. These spectra show Doppler-shifted γ-ray peaks. The data were obtained using proton windows A (upper spectra) and C (lower spectra). The arrows indicate peak centroids.

TABLE I. Doppler shifts and mean lives in V^{51}.

Transitions (MeV)	Observed $\Delta\langle E_\gamma\rangle$ (keV)	$F(\tau)_{\text{expt}}$	$\langle\tau\rangle$ (units of 10^{-13} sec)
1.609 $(\frac{11}{2}^-) \rightarrow 0$ $(\frac{7}{2}^-)$	5.55 ± 0.12	0.256 ± 0.006	6.3 ± 1.2
1.813 $(\frac{9}{2}^-) \rightarrow 0$ $(\frac{7}{2}^-)$	5.60 ± 0.21	0.231 ± 0.009	7.0 ± 1.4
2.402 $(\frac{3}{2}^-) \rightarrow 0$ $(\frac{7}{2}^-)$	31.8 ± 1.5	0.99 ± 0.04	
2.402 $(\frac{3}{2}^-) \rightarrow 0.320$ $(\frac{5}{2}^-)$	26.2 ± 1.4	0.94 ± 0.05	
	Average	0.975 ± 0.03	≤0.54
2.670 $(\frac{3}{2}^+) \rightarrow 0.430$ $(\frac{3}{2}^-)$	5.2 ± 0.5	0.22 ± 0.02	9 ± 2
2.699 $(\frac{15}{2}^-) \rightarrow 1.609$ $(\frac{11}{2}^-)$	−0.6 ± 1.2	−0.04 ± 0.08	≥11

cident beam direction. In order to stop elastically scattered beam particles, the proton detector was covered with a 0.05-mm aluminum foil. γ rays from the decay of excited states were detected in a 7.62-cm-long by 7.62-cm-diam cylindrical NaI(Tl) detector mounted on a turntable. The detector was positioned 8.2 cm from the target and was aligned so that the crystal axis passed through the center of the target. Data were taken at six angles between 0 and 90° relative to the beam direction.

We have used the analysis procedure described by Poletti and Warburton[15] for use with method II. In the reaction $Cr^{50}(\alpha, p\gamma)Mn^{53}$, utilization of collinear geometry leads to a particularly simple analysis. Since the only magnetic substates of Mn^{53} which can be populated in this geometry are $m = \pm\frac{1}{2}$, if the level spins are known, the only free parameter in the theoretical angular-correlation expression is the multipole mixing ratio. The theoretical distribution was fitted to the experimental distribution for various values of the multipole mixing ratio, δ, using a least-squares-fitting procedure. Curves of χ^2 (goodness of fit) versus $\tan^{-1}\delta$ were generated for each spin considered, and the best value of δ was taken to be the value for which a minimum χ^2 was obtained.

The theoretical expression used to fit the experimental distribution can be written as

$$W(\theta) = \sum_{\substack{k \\ \text{even}}} (A_k/A_0) P_k(\cos\theta) , \tag{2}$$

where $A_k/A_0 = f(\delta, \text{spins})$, and the $P_k(\cos\theta)$ are the Legendre polynomials. In this work, the spins are assumed fixed and only the lowest two multipole orders are considered, so we can write

$$A_k/A_0 = f(\delta) , \quad \text{or } \delta = F(A_k/A_0) . \tag{3}$$

Standard deviations in δ were then determined from the expression

$$\sigma_\delta = \frac{\partial F(A_2/A_0)}{\partial (A_2/A_0)} \sigma_{A_2/A_0} , \tag{4}$$

where σ_{A_2/A_0} is the standard deviation in A_2/A_0 determined by the least-squares-fitting procedure.

Method II requires that the reaction protons be detected at 0 or 180° with respect to the beam direction. In practice, however, the proton detector subtends a finite angle, and this allows the possibility of populating magnetic substates higher than $m = \pm\frac{1}{2}$. Following Litherland and Ferguson[5] we have estimated that the population of the $m = \pm\frac{3}{2}$ substate is less than 10% of the population of the $m = \pm\frac{1}{2}$ substate. Plots of χ^2 versus $\tan^{-1}\delta$ were

TABLE II. Comparison of V^{51} results with other work.

Level (MeV)	Transition (MeV)	Mean life (units of 10^{-13} sec)	$B(E2)_{\text{expt}}$ [a] (e^2 fm^4)	$B(E2)_{\text{expt}}$ [b] (e^2 fm^4)
1.609	1.61 $(\frac{11}{2}^-) \rightarrow 0.0$ $(\frac{7}{2}^-)$	6.3 ± 1.2	120 ± 25	83 ± 8
1.813	1.81 $(\frac{9}{2}^-) \rightarrow 0.32$ $(\frac{5}{2}^-)$	7.0 ± 1.4	39 ± 8	24 ± 5
	1.81 $(\frac{9}{2}^-) \rightarrow 0.0$ $(\frac{7}{2}^-)$	7.0 ± 1.4	42 ± 18	28 ± 5

[a] Present results. Branching ratios and multipole mixing ratio for the $\frac{9}{2}^- \rightarrow \frac{7}{2}^-$ transition are from Ref. 6.
[b] See Ref. 6.

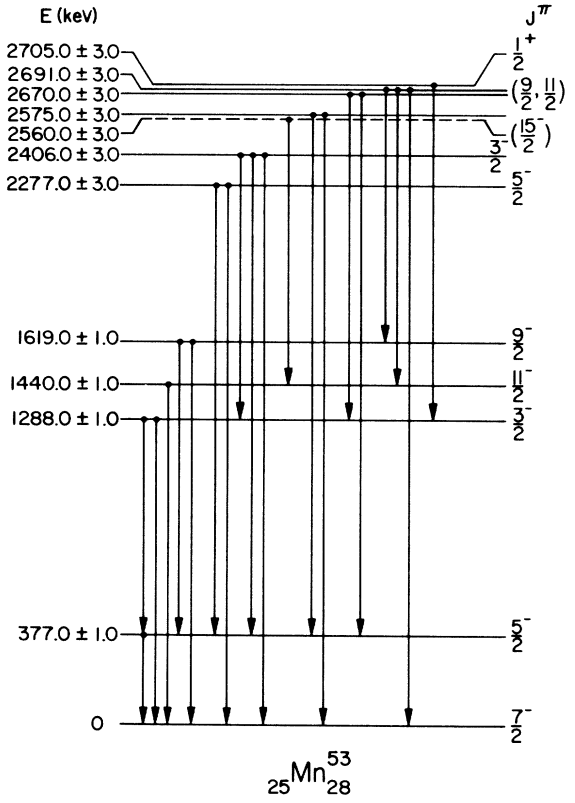

FIG. 5. Energy-level diagram for Mn^{53}. All known levels below 2.7 MeV are indicated. The γ-ray transitions shown are those observed in this work.

obtained in which a 10% population of the $m=\pm\frac{3}{2}$ substate was allowed. These curves are indicated on the χ^2 versus $\tan^{-1}\delta$ curves for comparison.

III. RESULTS

A. V^{51}

Figure 1 shows an energy-level diagram for V^{51}. The γ-ray transitions shown are those seen in this work. As mentioned above, branching ratios and angular correlations of many of the states in V^{51} formed in the reaction $Ti^{48}(\alpha,p)V^{51}$ have been previously measured,[6] so that we measured only mean lives of states in V^{51}. A proton spectrum resulting from the reaction $Ti^{48}(\alpha,p)V^{51}$ with 9.2-MeV α particles on an enriched $Ti^{48}O_2$ target is shown in Fig. 2. The resolution in this spectrum is about 90 keV, a factor of 2 better than that used in the Doppler-shift measurement. The proton windows used in the Doppler-shift measurements are indicated in the figure.

A spectrum of γ rays in coincidence with protons in window C is shown in Fig. 3. These γ rays were emitted at an angle of 150° with respect to the recoiling V^{51} nuclei. The proton window is primarily over states at 2.546, 2.670, and 2.699 MeV, but as can be seen, it also includes some protons to the 2.402-MeV state. The γ-ray peak at 1.609 MeV in Fig. 3 could correspond to a 2.546 → 0.926-MeV transition, but it can be explained as part of the 2.699 → 1.609 → 0 cascade,

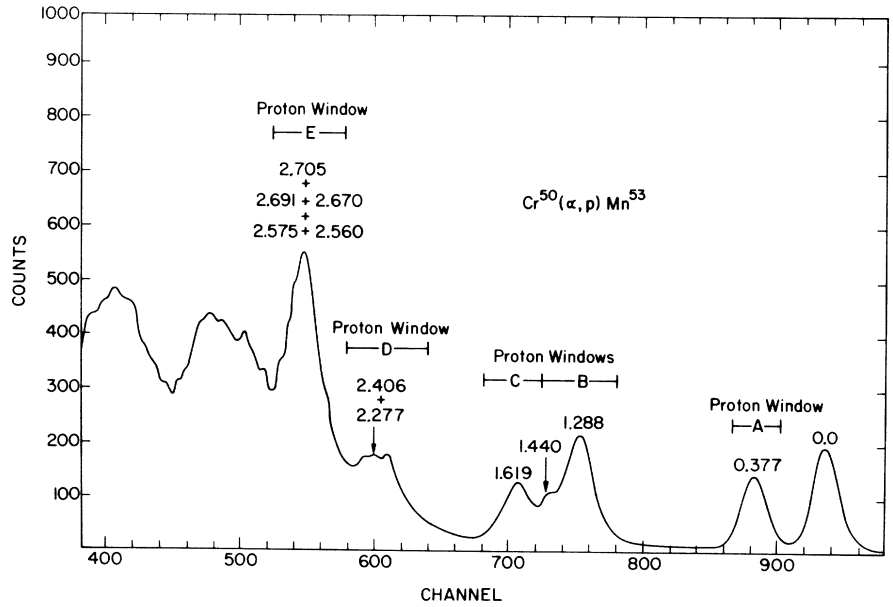

FIG. 6. Proton spectrum from the $Cr^{50}(\alpha,p)Mn^{53}$ reaction. The incident α-particle energy was 9.2 MeV and the target was Cr^{50} with an areal density of 250 $\mu g/cm^2$. Peaks are labeled with Mn^{53} level energies. Proton windows used in the Doppler-shift-attenuation and angular-correlation experiments are labeled.

TABLE III. Mn^{53} branching ratios.

Level energy (MeV)	Transition (MeV)	Branching ratio (%)	Other [a]
0.378 ± 1	0.378 → 0	100	100
1.288 ± 1	1.288 → 0	51 ± 1	49
	1.288 → 0.378	49 ± 1	51
1.440 ± 1	1.440 → 0	100	100
1.619 ± 1	1.619 → 0	90 [b]	83
	1.619 → 0.378	10 [b]	17
2.277 ± 3	2.277 → 0	74 ± 6	74
	2.277 → 0.378	26 ± 3	26
2.406 ± 3	2.406 → 0	29 ± 2	47
	2.406 → 0.378	12 ± 1	21
	2.406 → 1.288	59 ± 3	32
2.575 ± 3	2.575 → 0	27 ± 9 [b]	
	2.575 → 0.378	73 ± 14 [b]	
2.670 ± 3	2.670 → 0.378	67 ± 12 [b]	
	2.670 → 1.288	33 ± 5 [b]	
2.691 ± 3	2.691 → 0	52 ± 8 [b]	
	2.691 → 1.440	16 ± 3 [b]	
	2.691 → 1.619	32 ± 6 [b]	
2.705 ± 3	2.705 → 1.288	100	

[a] See Ref. 11.
[b] Based on relative peak areas at 90° only.

and we see no good evidence that the $\frac{1}{2}^+$ state at 2.546 MeV is populated. Figure 3 is a good example of the γ-ray spectra obtained in coincidence with protons to higher (above about 2 MeV) states in V^{51} and Mn^{53}. Figure 4 shows portions of spectra of γ rays emitted in forward (30°) and backward (150°) directions with respect to V^{51} nuclei. It is from these and similar spectra that the differences in energy in the numerator of Eq. (1) are obtained.

Our results for the mean lives of states in V^{51} are summarized in Table I. The errors in the mean lives shown in this table include an allowance for a 20% uncertainty in slowing-down powers. In Table II our results are compared with those of Horoshko, Cline, and Lesser. For the $\frac{9}{2}^- \rightarrow \frac{7}{2}^-$ transition we use the multipole mixing ratio from Ref. 6.

B. Mn^{53}

1. *Branching Ratios and Doppler Shifts*

Figure 5 shows an energy-level diagram of Mn^{53}. Again, the γ-ray transitions are those seen in this work. A proton spectrum resulting from the reaction $Cr^{50}(\alpha, p)Mn^{53}$ with 9.2-MeV α particles on an enriched Cr^{54} target 250 $\mu g/cm^2$ thick is shown in Fig. 6. The protons were detected in an annular

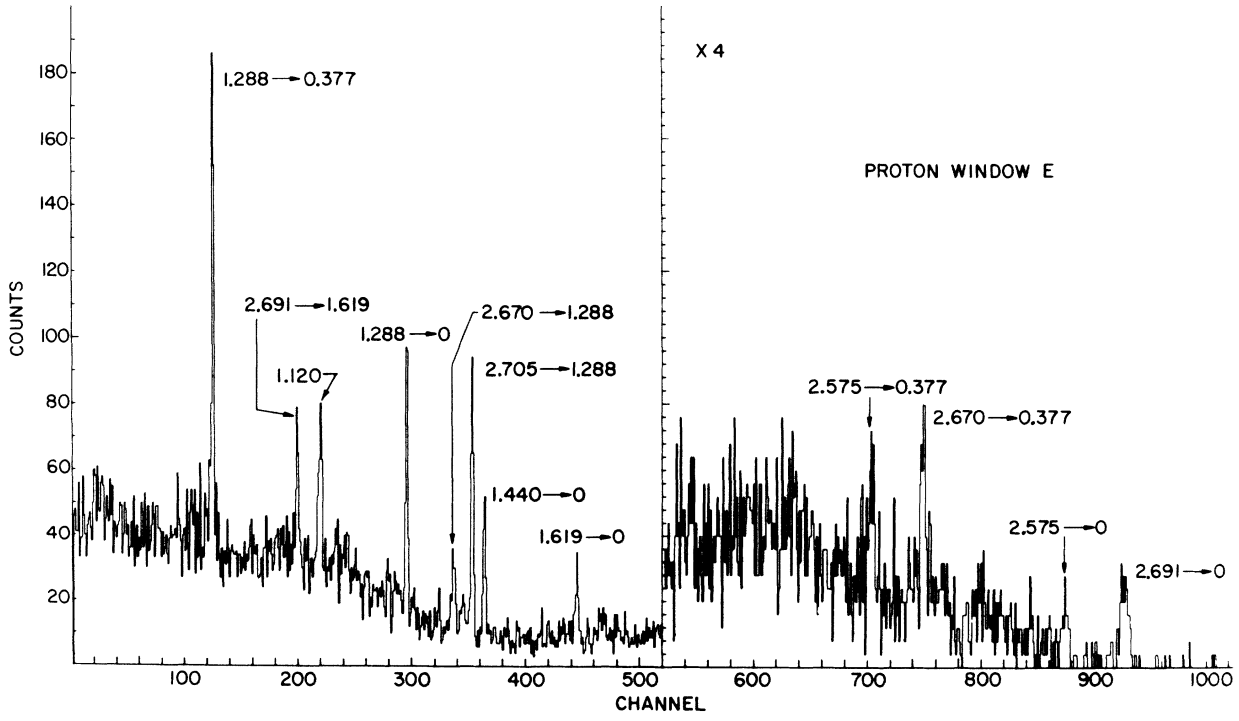

FIG. 7. Coincident γ-ray spectrum for Mn^{53}. These data were taken using proton window E (see Fig. 6), and with the Ge(Li) γ-ray detector positioned at 90° relative to the beam direction.

detector at an average angle of 155° with respect to the α-particle beam. The proton windows used in the Doppler-shift and angular-correlation measurements in Mn^{53} are shown. This spectrum is typical of those used in all of the Mn^{53} experiments; the width at half maximum of the proton peaks is about 160 keV. The cross section for this reaction was sensitive to α-particle energy, and it was possible to vary the relative proton yields to the two states in the window marked B in Fig. 6 in order to enhance the yield of the state of interest and suppress the other.

Figure 7 shows a spectrum of γ rays in coincidence with protons in window E of Fig. 6. γ rays

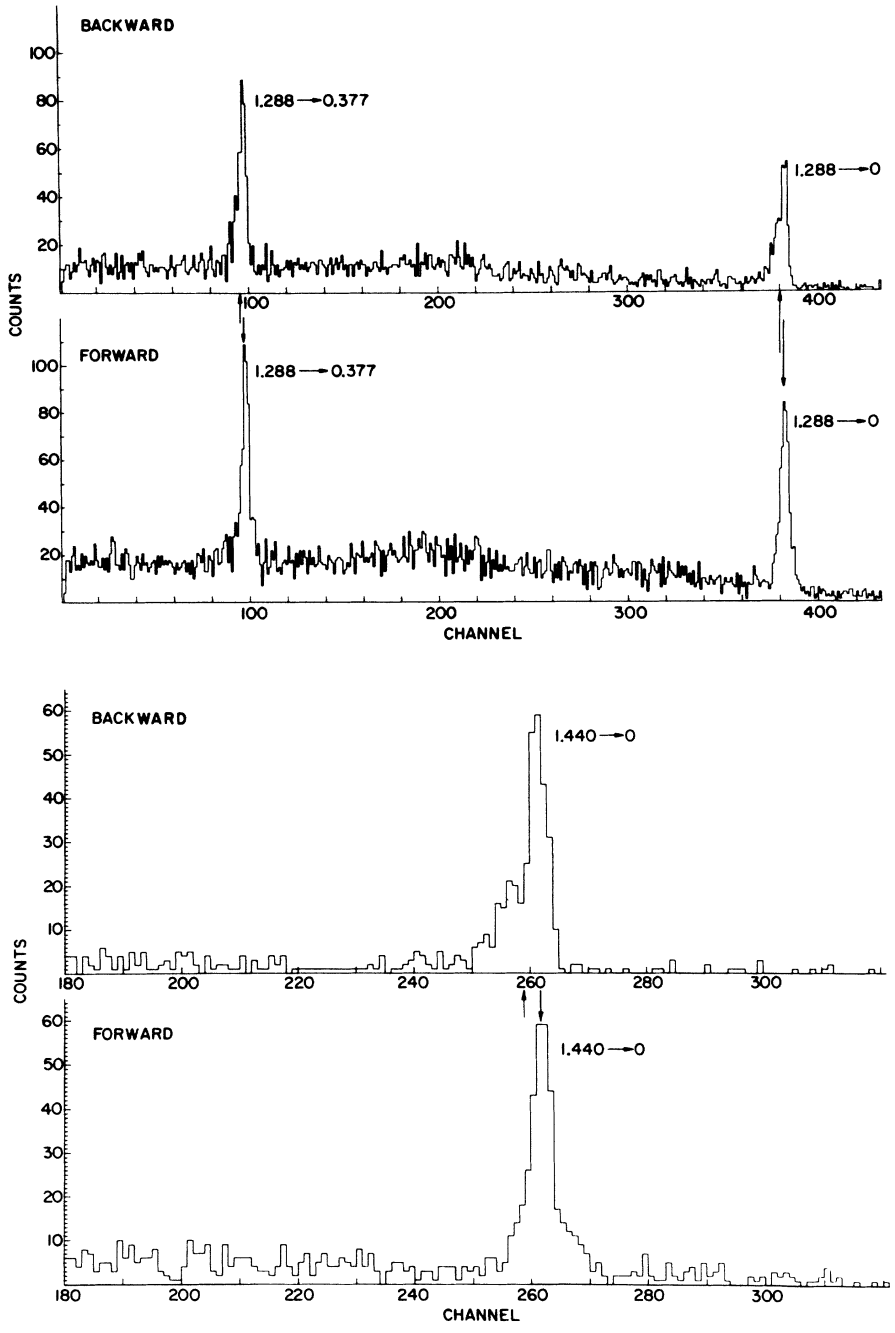

FIG. 8. Coincident γ-ray spectra for Mn^{53} for the transitions 1.288 MeV → 0, 1.288 → 0.378 MeV, and 1.440 MeV → 0. These spectra show experimentally observed Doppler shifts. The data were obtained using proton window B (see Fig. 6). The arrows indicate peak centroids.

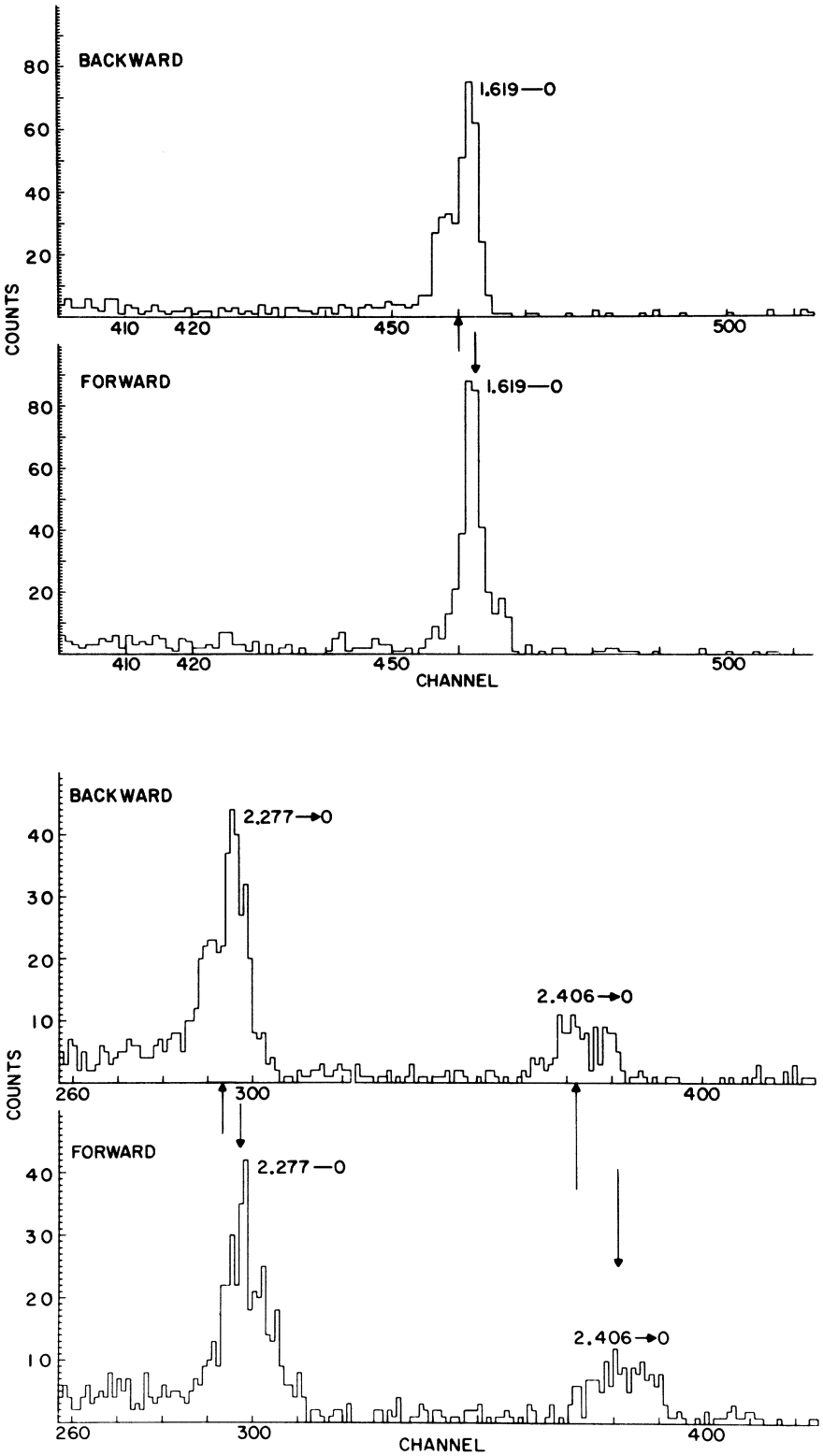

FIG. 9. Coincident γ-ray spectra for Mn^{53} for the transitions 1.619 MeV→0, 2.277 MeV→0, and 2.406 MeV→0. These spectra show Doppler-shifted γ-ray peaks. The data were obtained using proton windows C (upper spectra) and D (lower spectra). The arrows indicate peak centroids.

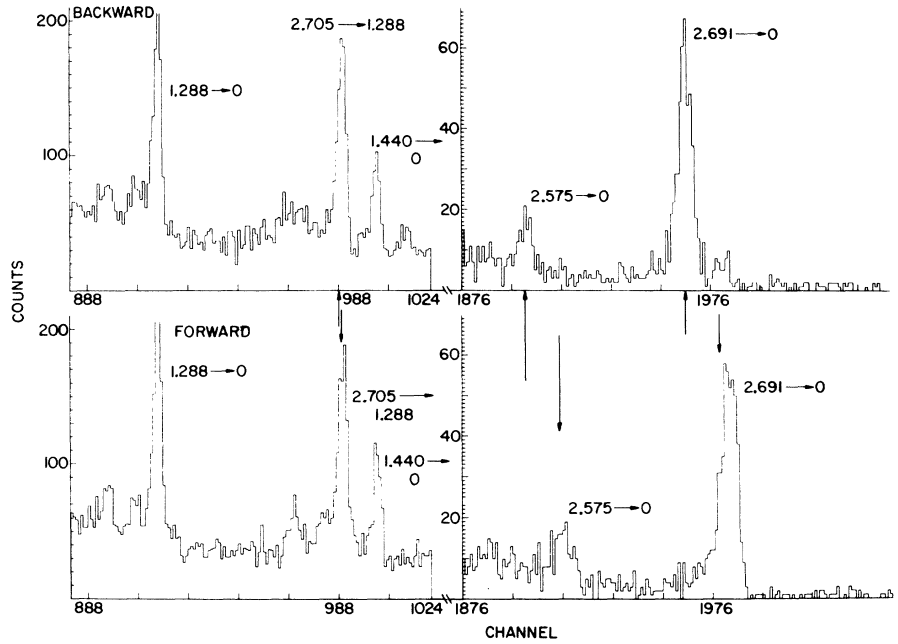

FIG. 10. Coincident γ-ray spectra for Mn^{53} for the transitions 2.575 MeV→0, 2.691 MeV→0, and 2.705→1.288 MeV. These spectra show Doppler-shifted γ-ray peaks. The data were obtained using proton window E (see Fig. 6). The arrows indicate peak centroids.

emitted in the decay of states at 2.705, 2.691, 2.670, and 2.575 MeV are in this spectrum. A γ-ray peak with an energy of 1.120 MeV also appears in the spectrum and will be discussed later. In Table III we list the energies and branching ratios of the lowest 10 states in Mn^{53} observed in this work. Those figures marked with a superscript b are based on spectra similar to that shown in Fig. 7, obtained with a Ge(Li) detector positioned at 90° with respect to the incident beam. The remainder of the branching ratios in the table were deduced from angular-correlation measurements made with a NaI γ-ray detector.

Figures 8 through 10 show portions of spectra of γ rays emitted forward (25°) and backward (150°) with respect to the direction of recoil of Mn^{53} ions. Differences in the energies of Doppler-shifted γ rays were deduced from these and simi-

TABLE IV. Doppler shifts and mean lives in Mn^{53}.

Transitions (MeV)	Observed $\Delta\langle E_\gamma\rangle$ (keV)	$F(\tau)_{\text{expt}}$	τ (units of 10^{-13} sec)	τ (units of 10^{-13} sec) [a]
1.288 ($\frac{3}{2}^-$)→0 ($\frac{7}{2}^-$)	2.9±0.5	0.17±0.03		
1.288 ($\frac{3}{2}^-$)→0.377 ($\frac{5}{2}^-$)	1.3±0.5	0.11±0.05		
	Average	0.16±0.03	$8.1^{+3}_{-2}{}^{+5}_{\cdot 5}$	8.7±2.2
1.440 ($\frac{11}{2}^-$)→0 ($\frac{7}{2}^-$)	3.0±0.5	0.15±0.03	8.1^{+3}_{-2}	11.5±3.8
1.619 ($\frac{9}{2}^-$)→0 ($\frac{7}{2}^-$)	4.14±0.41	0.186±0.019	$6.6^{+2}_{-1}{}^{+5}_{\cdot 5}$	5.6±1.5
2.277 ($\frac{5}{2}^-$)→0 ($\frac{7}{2}^-$)	7.4±0.6	0.25±0.02	$4.7^{+1}_{-1}{}^{+6}_{\cdot 0}$	
2.406 ($\frac{3}{2}^-$)→0 ($\frac{7}{2}^-$)	16.0±1.0	0.51±0.03	1.7±0.4	
2.575→0 ($\frac{7}{2}^-$)	24.4±1.3	0.741±0.043	0.7±0.3	
2.691→0 ($\frac{7}{2}^-$)	28.7±0.3	0.79±0.08 [b]	0.60±0.4	
2.705→1.288 ($\frac{3}{2}^-$)	2.08±0.4	0.12±0.2	11^{+4}_{-3}	

[a] See Ref. 7.

[b] Errors include a possible error due to the choice of limits in calculating the peak centroid.

TABLE V. Experimental angular-correlation results for Mn^{53}.

Transition (MeV)	A_2/A_0	A_4/A_0
0.378 → 0.0	−0.76 ± 0.02	0.03 ± 0.02
1.288 → 0.0	0.01 ± 0.03	00.0
1.288 → 0.377	−0.25 ± 0.03	00.0
1.440 → 0.0	0.9 ± 0.1	0.18 ± 0.12
1.619 → 0.0	0.24 ± 0.04	0.30 ± 0.04
2.277 → 0.0	−0.32 ± 0.07	0.1 ± 0.1
2.406 → 0.0	0.26 ± 0.11	00.0
2.406 → 1.288	0.58 ± 0.07	00.0
2.705 → 1.288	0.06 ± 0.06	00.0

lar spectra, and are tabulated, together with mean lives derived from them, in Table IV. The errors in the mean lives shown in this table include an allowance for a 20% uncertainty in the slowing-down properties of the material through which the Mn^{53} nuclei recoil. Also shown in the table are some recently published results of Brandolini *et al.*[7]

2. *Angular Correlations*

The experimental results of the proton–γ-ray angular-correlation measurements are listed in Table V. The multipole mixing ratios obtained from these results are listed in the second column of Table VI. To obtain these mixing ratios from the results in Table V, we have assumed that the spins and parities of states in Mn^{53} up to 2 MeV are known, and are those shown in Fig. 5. The adopted values of multipole mixing ratios listed in the last column of Table VI are the averages of all of the individual measurements. Simple averages were taken since the significance of the errors quoted with individual measurements is not clear. For example, our errors are standard deviations; whereas, those of Szöghy, Cujec, and Dayrus[11] were deduced from the spread of δ at a χ^2 value corresponding to a 0.1% confidence limit in a plot of χ^2 versus $\tan\delta$. The uncertainties in the adopted values are those from this work, and are standard deviations. Arguments used to select a particular value of δ rather than other possible solutions are presented below.

(i) 0.378-MeV ($\frac{5}{2}^-$) → 0.0-MeV ($\frac{7}{2}^-$) transition. Our results are consistent with two different values of δ. However, Vuister[9] has eliminated one possibility with a measurement of the polarization of 0.378-MeV γ rays.

(ii) 1.288-MeV ($\frac{3}{2}^-$) → 0.378-MeV ($\frac{5}{2}^-$) transition. If the larger value of $\delta(+12)$ is used for this transition, the strength of the $E2$ part of the transition is $|M(E2)|^2 = \Gamma_{expt}(E2)/\Gamma_W(E2) = 67^{+30}_{-20}$, where Γ_W is calculated from the equation given by Wilkinson.[16] The larger value of δ also gives $|M(M1)|^2 = 2^{+5}_{-1} \times 10^{-4}$. The smaller value of $\delta(-0.15)$ gives $|M(E2)|^2 = 1.5^{+1.5}_{-0.8}$ and $|M(M1)|^2 = 2.5 \pm 0.9 \times 10^{-2}$. On the basis of the $E2$ strengths, we would prefer the smaller value of δ. Horoshko, Cline, and Lesser[6] in V^{51} chose the larger of their two possible values of δ. From data presently available, it is not possible to make a definite choice, and both values of δ are listed in Table VI.

TABLE VI. Multipole mixing ratios in Mn^{53}.

Transition (MeV)	Present results	Ref. 8	Ref. 9	Ref. 10	Ref. 11		Adopted values
0.378 ($\frac{5}{2}^-$) → 0 ($\frac{7}{2}^-$)	−0.53 ± 0.03	−0.6 ± 0.3	−0.61 ± 0.08	−0.46 ± 0.11	−0.27 ± 0.08		
	−2.36 ± 0.02	$-2.4^{\pm\frac{1}{2}}$			$-7.6^{\pm\frac{3}{7}}$		−0.49 ± 0.03
1.288 ($\frac{3}{2}^-$) → 0.378 ($\frac{5}{2}^-$)	−0.14 ± 0.03		−0.18 ± 0.03	−0.21 ± 0.08	$-0.09^{+0.09}_{-0.12}$		−0.15 ± 0.03
	+14 ± 6		30^{+27}_{-15}	−1.7 ± 0.2	$1.73^{\pm1.0}_{-0.7}$	or	12 ± 6
1.619 ($\frac{3}{2}^-$) → 0 ($\frac{7}{2}^-$)	−0.31 ± 0.03				$-0.5^{\pm0.2}_{-0.4}$		−4.9 ± 1
	−8 ± 1	−3.2 ± 1			$-3.5^{\pm1}_{-3.5}$		
2.277 ($\frac{5}{2}^-$) → 0 ($\frac{7}{2}^-$)	−0.12 ± 0.05				−0.26 ± 0.08		−0.17 ± 0.05
	∞				-6.7^{+2}_{-3}	or	≤−5
2.406 ($\frac{3}{2}^-$) → 1.288 ($\frac{3}{2}^-$)	−0.16 ± 0.05				−0.1 ± 0.1		−0.13 ± 0.05
	−2.4 ± 0.3				-54^{+3}_{-15}		
2.691 → 0 ($\frac{7}{2}^-$)	Not determined						
2.705 ($\frac{1}{2}^+$) → 1.288 ($\frac{3}{2}^-$)	Not determined						

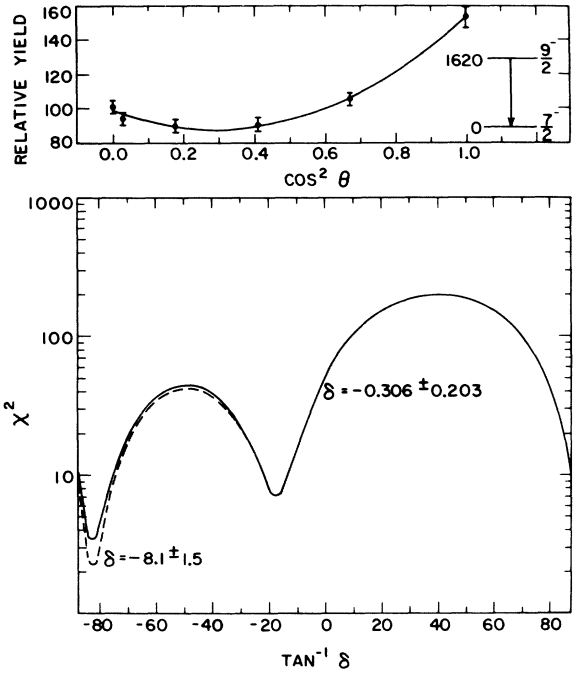

FIG. 11. Angular-correlation results for the Mn^{53} transition 1.619 MeV $(\frac{9}{2}^-) \rightarrow 0$ $(\frac{7}{2}^-)$. The best fit to the data, and the χ^2 versus $\tan^{-1}\delta$ curve are shown. The dashed curve is for $P(\frac{3}{2}) = 0.1P(\frac{1}{2})$.

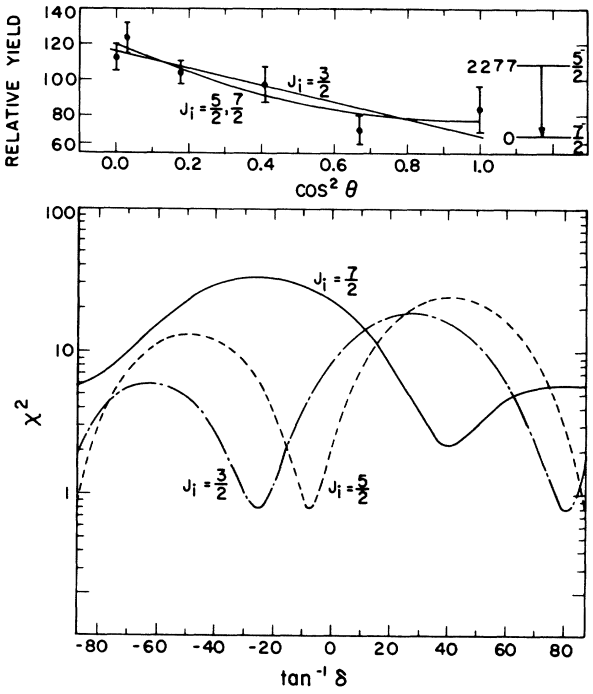

FIG. 12. Angular-correlation results for the Mn^{53} transition 2.277 MeV$\rightarrow$0 $(\frac{7}{2}^-)$. Best fits to the data for $J(2.277) = \frac{3}{2}$, $\frac{5}{2}$, and $\frac{7}{2}$, and the χ^2 versus $\tan^{-1}\delta$ curves for these spin possibilities are shown.

(iii) 1.619-MeV $(\frac{9}{2}^-) \rightarrow$ 0.0-MeV $(\frac{7}{2}^-)$ transition. Figure 11 shows a plot of χ^2 versus δ for this transition. It can be seen that the large negative value of δ is more probable than the low one. The data of McEllistrem, Jones, and Sheppard[8] favor the large negative value of δ to such an extent that they do not quote the smaller one.

(iv) 2.277-MeV $\rightarrow$ 0.0-MeV $(\frac{7}{2}^-)$ transition. Our angular-correlation results for this state are shown in Fig. 12. The most likely spins for this state are $\frac{3}{2}$, $\frac{5}{2}$, or $\frac{7}{2}$, although the assignment of $\frac{7}{2}$ is less probable than the other two. The data of Szöghy, Cujec, and Dayrus[11] are consistent with spins of $\frac{3}{2}$ or $\frac{5}{2}$. McEllistrem[17] has information which indicates that this state has a spin of $\frac{5}{2}$ or $\frac{7}{2}$. Therefore the most likely spin for this state is $\frac{5}{2}$. If the parity of the state were positive, our multipole mixture (from Table VI) and mean

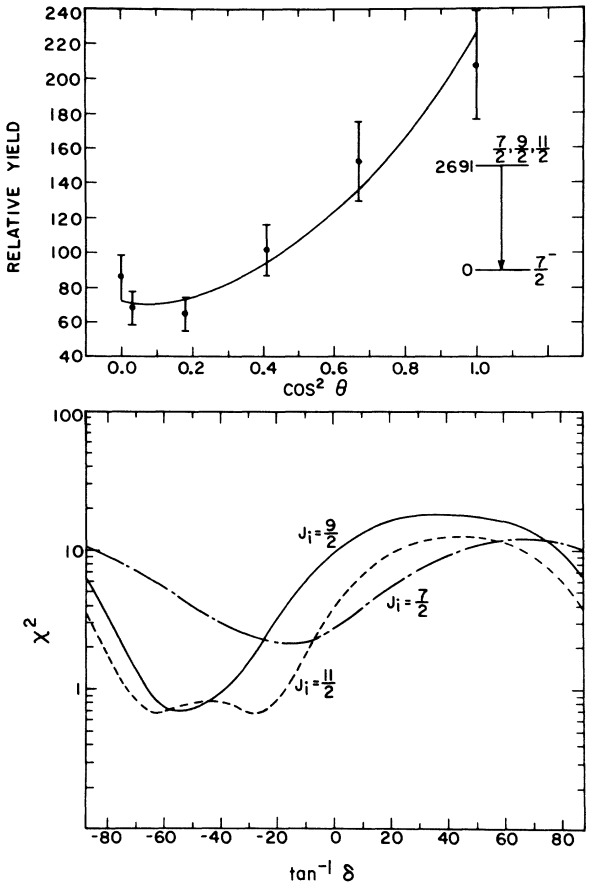

FIG. 13. Angular-correlation results for the Mn^{53} transition 2.691 MeV$\rightarrow$0$(\frac{7}{2}^-)$. Best fits to the data for $J(2.691) = \frac{7}{2}$, $\frac{9}{2}$, and $\frac{11}{2}$, and the χ^2 versus $\tan^{-1}\delta$ curves for these spin possibilities are shown. Results for $J(2.691) = \frac{5}{2}$ are no better than those for $J(2.691) = \frac{7}{2}$, and they are not shown.

TABLE VII. Experimental $M1$ transition strengths.

Transition	Nucleus	Energy (MeV)	$\lvert M(M1)\rvert^2 = \frac{\Gamma_{\text{expt}}(M1)}{\Gamma_W(M1)}$
$\frac{5}{2}^- \rightarrow \frac{7}{2}^-$	V^{51}	$0.320 \rightarrow 0.0$	$3.3 \pm 0.3 \times 10^{-3}$ [a]
	Mn^{53}	$0.378 \rightarrow 0.0$	$2.8 \pm 6.3 \times 10^{-3}$ [b]
$\frac{3}{2}^- \rightarrow \frac{5}{2}^-$	V^{51}	$0.930 \rightarrow 0.320$	$1.5 \pm 0.2 \times 10^{-3}$ [c] or $1.9^{+1.5}_{-0.7} \times 10^{-5}$
	Mn^{53}	$1.288 \rightarrow 0.378$	$2.5 \pm 0.9 \times 10^{-2}$ [d] or $2^{+5}_{-1} \times 10^{-4}$
$\frac{9}{2}^- \rightarrow \frac{7}{2}^-$	V^{51}	$1.813 \rightarrow 0.0$	$3.7 \pm 1.5 \times 10^{-4}$
	Mn^{53}	$1.619 \rightarrow 0.0$	$3.7 \pm 1.7 \times 10^{-4}$

[a] See Refs. 6 and 20.
[b] Mean life of 0.378-MeV state is from Ref. 1.
[c] See Ref. 6.
[d] Using smallest of two possible multipole mixing ratios.

life (from Table IV) would give a 2.277 → 0.0-MeV transition which was either a pure $M2$ or an $E1$ transition with a strength of $|M(E1)|^2 = 10^{-4}$. If the state has negative parity, the multipole mixture $\delta = -0.17$ would give $|M(E2)|^2 = 0.06$, a value too small to be acceptable. For negative parity and $\delta \leq -5$, we obtain $|M(E2)|^2 = 1.8 \pm 0.4$ and $M(M1) \leq 1.5 \times 10^{-4}$. This latter possibility, negative parity and $\delta \leq -5$, seems to be the most likely one, but it is not possible to rule out positive parity and $\delta = -0.17$.

(v) 2.406 → 1.288-MeV ($\frac{3}{2}^-$) transition. This state has been shown to be an $l=1$ state,[18] and the fact that the proton-γ-ray correlation is nonisotropic fixes its quantum numbers as $\frac{3}{2}^-$. For this transition, the smaller value of $|\delta|$ gives reasonable values for the transition strengths, namely, $|M(M1)|^2 = 7.5 \pm 2 \times 10^{-2}$, and $|M(E2)|^2 = 2.2 \pm 0.5$.

(vi) 2.691-MeV state. Our angular-correlation results for the transition from this state to ground are shown in Fig. 13. They are consistent with spins of $\frac{9}{2}$, $\frac{11}{2}$, and perhaps, $\frac{7}{2}$. If the spin of the state were $\frac{11}{2}$, the $E2$ transition to the ground would have an enhancement of 7. Chung, Olsen, and Sheppard[19] have assigned a tentative spin of $\frac{9}{2}$ to this level.

(vii) 2.705-MeV state. Cujec and Szöghy[18] have observed an $l=0$ state at 2.720 ± 0.010 MeV. Our angular-correlation results for the 2.705-MeV state are isotropic. Further, we observe the decay of this state only to the $\frac{3}{2}^-$, 1.288-MeV state. It seems probable that this state is the $\frac{1}{2}^+$, $l=0$

TABLE VIII. Comparison of transition probabilities in V^{51} and Mn^{53}.

Transition	σL	$\lvert M\rvert^2$ V^{51}	$\lvert M\rvert^2$ Mn^{53}	Ratio (Mn^{53}/V^{51})
$\frac{5}{2}^- \rightarrow \frac{7}{2}^-$	$M1$	$3.3 \pm 0.3 \times 10^{-3}$	$2.8 \pm 0.3 \times 10^{-3}$	0.85 ± 0.15
	$E2$	11.4 ± 0.8	10.6 ± 1.5	0.93 ± 0.16
$\frac{3}{2}^- \rightarrow \frac{7}{2}^-$	$E2$	6.6 ± 0.4	11.8 ± 4	1.9 ± 0.6
$\frac{3}{2}^- \rightarrow \frac{5}{2}^-$	$M1$	$1.5 \pm 0.2 \times 10^{-3}$	$2.5 \pm 0.9 \times 10^{-2}$	17^{+9}_{-7} [a]
		or $2.0^{+1.3}_{-0.8} \times 10^{-5}$	$2^{+5}_{-1} \times 10^{-4}$	10^{+11}_{-6} [b]
	$E2$	$1.0^{+0.8}_{-0.4}$	$1.5^{+1.5}_{-0.8}$	$1.5^{+1.6}_{-0.9}$ [a]
		or 9.4 ± 0.8	67^{+30}_{-20}	$7^{+4}_{-2.5}$ [b]
$\frac{11}{2}^- \rightarrow \frac{7}{2}^-$	$E2$	9.8 ± 0.2	13.4 ± 4.0	1.4 ± 0.3 [c]
$\frac{9}{2}^- \rightarrow \frac{7}{2}^-$	$M1$	$3.7 \pm 1.5 \times 10^{-4}$	$3.7 \pm 1.7 \times 10^{-4}$	1.0 ± 0.6 [c]
	$E2$	3.6 ± 1.0	7.0 ± 1.7	1.9 ± 0.3 [c]
$\frac{9}{2}^- \rightarrow \frac{5}{2}^-$	$E2$	3.4 ± 0.7	5.5 ± 1.4	1.6 ± 0.3 [c]

[a] Using small value for multipole mixing ratio.
[b] Using large value for multipole mixing ratio.
[c] These errors do not include stopping-power uncertainties.

state seen by Cujec and Szöghy.[18] The transition is then most likely an $E1$ transition with a strength $|M(E1)|^2 = 2.2 \pm 0.5 \times 10^{-4}$.

In addition to the values of multipole mixing ratios listed in the table, we have measured multipole mixtures of all $\Delta J = 2$, no, transitions among the states below 2.5 MeV and found them to be consistent with pure $E2$ radiation.

3. 2.560-MeV State

As mentioned above, the γ-ray spectrum illustrated in Fig. 7 contains a 1.120-MeV γ-ray peak whose origin is not obvious. In addition, this spectrum contains a γ-ray peak at 1.440 MeV, produced by γ rays emitted in the transition from the $\frac{11}{2}^-$, 1.440-MeV state to the ground state. We have tried to explain the intensity of this 1.440-MeV peak by considering all possible ways of populating that state. The data in Fig. 7 seem to be consistent only with the assumption that a state at 2.560 MeV is produced in the reaction $Cr^{50}(\alpha, p)Mn^{53}$, and decays to the 1.440-MeV state, emitting a 1.120-MeV γ ray. We could find no other reasonable explanation for the existence and size of these two peaks. Such a state could be the $\frac{15}{2}^-$ member of the $(f_{7/2})^{-3}$ multiplet. The $\frac{15}{2}^-$ state in V^{51} is populated by the reaction $Ti^{48}(\alpha, p)V^{51}$ with 10-MeV α particles, as is evidenced by the 2.699 → 1.609-MeV transition shown in Fig. 3. Therefore, it would not be surprising if the $\frac{15}{2}^-$ state in Mn^{53} were populated in our experiment.

IV. DISCUSSION

In all of the results quoted in this section, multipole mixing ratios and branching ratios in V^{51} and the $E2$ transition strength of the 0.93-MeV state in V^{51} are taken from Horoshko, Cline, and Lesser.[6] The mean life of the 320-keV state in V^{51} is from Shipley, Holland, and Lynch,[20] and of the 378-keV state in Mn^{53} is from Goredetsky *et al.*[21] For all other numbers, the results quoted in Tables I, IV, and VI are used.

TABLE IX. $B(E2)\downarrow$; calculated and measured (e^2 fm^4).

Transition	V^{51}	Mn^{53}	Calc.
$\frac{5}{2}^- \rightarrow \frac{7}{2}^-$	154 ± 7.6 [a]	122 ± 18 [b]	196
$\frac{3}{2}^- \rightarrow \frac{7}{2}^-$	76 ± 5 [a]	143 ± 50	69
$\frac{3}{2}^- \rightarrow \frac{5}{2}^-$	107 ± 9 or 11^{+9}_{-6} [a]	814^{+360}_{-230} or 18^{+18}_{-9}	51
$\frac{11}{2}^- \rightarrow \frac{7}{2}^-$	101 ± 20 [c]	160 ± 50	90
$\frac{9}{2}^- \rightarrow \frac{7}{2}^-$	35 ± 6 [c]	85 ± 22	33
$\frac{9}{2}^- \rightarrow \frac{5}{2}^-$	32 ± 6 [c]	64 ± 16	31

[a] See Ref. 6.
[b] Mean life from Ref. 21.
[c] Average from this work and Ref. 6.

The predictions of the shell model which provide a sensitive test of the model's applicability to V^{51} and Mn^{53} are those which concern the electromagnetic transition properties of these nuclei. In particular, two predictions which result from the shell-model treatment of V^{51} and Mn^{53} are: (1) If configuration mixing is not allowed [that is, if pure $(1f_{7/2})^n$ wave functions are used] then all $M1$ transitions between states are forbidden; and (2) since particles and "holes" are treated identically, the electromagnetic transition properties of V^{51} and Mn^{53} should be identical.

Experimental $M1$ transition strengths for V^{51} and Mn^{53} are shown in Table VII. This table includes only those levels which may reasonably be expected to be $(1f_{7/2})^n$ levels. While the existence of even very small $M1$ transition strengths for these levels requires some configuration mixing, the experimental $M1$ strengths are generally small and in good agreement with the simple pure-configuration model. A possible exception to this agreement is the $\frac{3}{2}^- \rightarrow \frac{5}{2}^-$ transition in Mn^{53}. For one of the possible multipole mixing ratios, this transition is less than a factor of 10 slower than most allowed $M1$ transitions, and implies some configuration mixing in the initial and final states. Because of the proximity of the $2p_{3/2}$ and $1f_{5/2}$ levels to the $1f_{7/2}$ level, the $\frac{3}{2}^-$ and $\frac{5}{2}^-$ states with predominantly $(1f_{7/2})^n$ configurations are more likely to contain configuration mixing than other $(1f_{7/2})^n$ states. Thus transitions between these two states might be expected to have a larger $M1$ component than transitions between other $(1f_{7/2})^n$ states.

Table VIII includes a comparison of the electromagnetic transition properties of V^{51} and Mn^{53} with respect to their respective $M1$ and $E2$ transition strengths. This table also includes only those

TABLE X. Comparison of mean lives with mixed-configuration calculation.

Level	E (MeV)	τ_{calc} (units of 10^{-13} sec)	τ_{expt} (units of 10^{-13} sec)
$\frac{3}{2}^-$	1.288	48.2	8.1 ± 3.0
$\frac{11}{2}^-$	1.440	20.5	8.1 ± 2.5
$\frac{9}{2}^-$	1.619	11.1	6.6 ± 2.0
$\frac{5}{2}^-$	2.277	0.2	4.7 ± 1.3
$\frac{3}{2}^-$	2.406	2.4	1.7 ± 0.5
$\frac{7}{2}^-$ (?)	2.575	3.4	0.72 ± 0.28

levels which are expected to have predominantly $(1f_{7/2})^n$ configurations. One value of the comparison presented in Table VIII is that most of the measurements on the two nuclei were made in the same laboratory, using the same techniques. An appreciable fraction of the errors in individual transition probabilities stems from uncertainties in stopping powers used to calculate mean lives from Doppler-shift attenuations, and errors from this source tend to cancel in the ratios presented in the last column of the table. As can be seen from the table, the agreement between most of the corresponding transition rates in the two nuclei is remarkable. The only transitions in which there is a significant difference in the rates for the two nuclei are those between the $\frac{3}{2}^-$ and $\frac{5}{2}^-$ states. From an inspection of this table, we would prefer to choose the smaller of the possible multipole mixing ratios for the $\frac{3}{2}^- \rightarrow \frac{5}{2}^-$ transition. This choice would yield $E2$ rates in the two nuclei which were equal. The lack of agreement of the $M1$ rates could then be attributed to a slight difference in the admixture of $2p_{3/2}$ and $1f_{5/2}$ components in the $\frac{3}{2}^-$ and $\frac{5}{2}^-$ states in the two nuclei. It should be noted, however, that Horoshko, Cline, and Lesser[6] chose the larger of the possible multipole mixing ratios for V^{51}.

A third comparison with the $(1f_{7/2})^n$ shell-model calculation is presented in Table IX. In this table, calculated and measured $B(E2)$ values are compared. For the calculated $B(E2)$'s an effective charge for the proton of $e' = 1.7e$ and for the neutron of $e' = 1.0e$ were used, together with a value for $r^2 = 19.2$ fm.[2] These values were not chosen just to fit the V^{51} and Mn^{53} data, but are those which give reasonable fits to experimental results throughout the $f_{7/2}$ shell.[2] The agreement between calculation and experiment presented in Table IX is not perfect, but considering the simplicity of the model used in the calculations, it is quite good.

Finally, mean lives of negative-parity states in Mn^{53} have been calculated with a mixed-configuration model[3] which allows small $2p_{3/2}$ and $1f_{5/2}$ admixtures to the $1f_{7/2}$-shell states. We compare the results of our experiment with those calculations in Table X.

In summary, we have studied in detail the strengths of electromagnetic transitions among the low-energy states of Mn^{53} and V^{51}. For levels below 2 MeV which can reasonably be identified with $(1f_{7/2})^n$ configurations our results show: (a) $M1$ transitions are inhibited by factors of from 50 to 50 000. These inhibitions generally are much greater than are found in ordinary $M1$ transitions; (b) corresponding transitions in V^{51} and Mn^{53} agree very well; and (c) $B(E2)$ values from shell-model calculations using $(1f_{7/2})^n$ configurations agree quite well with experimental results. For energies greater than 2 MeV many levels occur and cannot be accounted for with the simple $(1f_{7/2})^n$ configurations. Comparison of our measured mean lives with some calculated using mixed configurations shows reasonable agreement in most cases.

The authors are happy to acknowledge many conversations with J. D. McCullen concerning the material in this paper. Professor McCullen also calculated the $B(E2)$'s listed in Table IX.

---

†Work supported in part by U. S. Atomic Energy Commission.

[1]I. Talmi, Phys. Letters 25B, 313 (1967).
[2]J. D. McCullen, private communication.
[3]K. Lipps and M. T. McEllistrem, Phys. Rev. C 1, 1009 (1970); K. Lipps, Phys. Rev. C 4, 1482 (1971).
[4]R. L. Hershberger, M. J. Wozniak, Jr., and D. J. Donahue, Phys. Rev. 186, 1167 (1969).
[5]A. E. Litherland and A. J. Ferguson, Can. J. Phys. 39, 788 (1961).
[6]R. N. Horoshko, D. Cline, and P. M. S. Lesser, Nucl. Phys. A149, 562 (1970).
[7]F. Brandolini, A. Brusegan, R. A. Ricci, and C. Signorini, Topical Conference on the Structure of $1f_{7/2}$ Nuclei, Padua, Italy, 1971 (unpublished).
[8]M. T. McEllistrem, K. W. Jones, and D. M. Sheppard, Phys. Rev. C 1, 1409 (1970).
[9]P. H. Vuister, Nucl. Phys. A91, 521 (1967).
[10]S. Gorodetzky, F. A. Beck, R. Bertini, E. Bozek, and A. Knipper, Nucl. Phys. 85, 576 (1966).
[11]I. M. Szöghy, B. Cujec, and R. Dayrus, Nucl. Phys. A153, 529 (1970).
[12]M. J. Wozniak, Jr., and D. J. Donahue, Phys. Rev. C 1, 601 (1970).
[13]J. Lindhard, M. Scharff, and H. E. Schiøtt, Kgl. Danske Videnskab. Selskab, Mat.-Fys. Medd. 33, No. 14 (1963).
[14]A. E. Blaugrund, Nucl. Phys. 88, 501 (1966).
[15]A. R. Poletti and E. K. Warburton, Phys. Rev. 137, B595 (1965).
[16]D. H. Wilkinson, in *Nuclear Spectroscopy*, edited by F. Ajzenberg-Selove (Academic, New York, 1960).
[17]M. T. McEllistrem, private communication.
[18]B. Cujec and I. M. Szöghy, Phys. Rev. 179, 1060 (1969).
[19]W. H. Chung, W. C. Olsen, and D. M. Sheppard, Bull. Am. Phys. Soc. 15, 784 (1970).
[20]E. N. Shipley, R. E. Holland, and F. J. Lynch, Phys. Rev. 182, 1165 (1969).
[21]S. Gorodetzky, N. Schulz, E. Bozek, and A. Knipper, Nucl. Phys. 85, 519 (1966).